

# Structure of the Dimethyl Ether–CO<sub>2</sub> van der Waals Complex from Microwave Spectroscopy

Josh J. Newby, Rebecca A. Peebles, and Sean A. Peebles\*

Department of Chemistry, Eastern Illinois University, 600 Lincoln Avenue, Charleston, Illinois 61920

Received: August 6, 2004; In Final Form: October 6, 2004

The rotational spectrum of the 1:1 weakly bound complex formed between dimethyl ether (DME) and CO<sub>2</sub> has been assigned by Fourier transform microwave spectroscopy, leading to rotational constants of  $A = 5401.24(11)$  MHz,  $B = 2010.8637(17)$  MHz, and  $C = 1493.4844(15)$  MHz for the normal isotopic species. Measurement of rotational spectra for an additional four isotopomers has allowed a structure determination for this complex, giving a  $C_{2v}$  geometry in which the CO<sub>2</sub> lies in the heavy atom plane of the DME and is aligned perpendicular to its  $C_2$  axis. This orientation is supported by second moment data and a dipole moment of  $\mu_a = \mu_{\text{total}} = 1.661(6)$  D. The C $\cdots$ O distance has been determined to be 2.711(1) Å. Ab initio optimizations at the MP2/6-311++G(2d,2p) level predict a  $C_{2v}$  geometry with a C $\cdots$ O bond length of 2.685 Å, slightly shorter than, but still in very good agreement with, the experimental value. Predicted rotational constants and dipole moment at this level of theory are  $A = 5379$  MHz,  $B = 2018$  MHz,  $C = 1495$  MHz, and  $\mu_a = 1.83$  D.

## Introduction

There have been several recent spectroscopic studies of complexes involving C–H hydrogen bonding interactions.<sup>1–3</sup> These investigations allowed unambiguous determination of the structures of these weakly bound species, usually via Fourier transform microwave spectroscopy,<sup>1,2</sup> although some studies by the Caminati group have also utilized free-jet millimeter wave spectroscopy.<sup>1,3</sup> Numerous investigations in the past few years have centered on clusters involving the dimethyl ether (DME) molecule which is well suited for the formation of C–H hydrogen bonding interactions due to the location of two methyl groups next to an electronegative ether oxygen atom. Dimethyl ether complexes studied to date include DME dimer,<sup>1</sup> DME–HF,<sup>4</sup> DME with doubly and triply fluorinated ethylenes,<sup>2</sup> and DME complexes with the rare gas atoms Ne,<sup>5</sup> Ar,<sup>6</sup> Kr,<sup>7</sup> and Xe.<sup>8</sup> With the exception of the rare gas complexes, all of these dimers involve complexation of DME with another proton donating species. In our laboratory we recently assigned the rotational spectra of five isotopomers of the DME–OCS complex,<sup>9</sup> in which the DME is the only possible proton donor. This dimer was shown to have a heavy atom planar structure in which the OCS lies in the COC plane of the DME, and is crossed relative to its  $C_2$  axis making an O $\cdots$ C=S angle of 96.5(2)°.<sup>9</sup>

As part of an ongoing systematic characterization of complexes that have the potential to exhibit C–H hydrogen bonding interactions, an obvious extension was to study the DME–CO<sub>2</sub> complex. Previous work on this dimer was carried out in the IR in 2003 by van Ginderen, et al.<sup>10</sup> who isolated the dimer in liquid Ar and also carried out some ab initio calculations. Their IR investigation identified blue shifts, in the range 0 to 5 cm<sup>-1</sup>, in the C–H stretching frequencies of the complex relative to the monomer; these shifts would be consistent with formation of C–H hydrogen bonding interactions between the DME and

CO<sub>2</sub>. The ab initio calculations performed in the 2003 study<sup>10</sup> included explicit consideration of basis set superposition error (BSSE) in the structure optimizations by using the CP-corrected gradient techniques of Simon, et al.<sup>11</sup> and predicted a C $\cdots$ O van der Waals bond length of 2.812 Å. This is about 0.1 Å shorter than the corresponding experimental distance of 2.916(3) Å determined for the DME–OCS complex,<sup>9</sup> indicating either a decrease in steric interactions when the large sulfur atom is removed from the system, or possibly an increase in the binding energy of the system due to the replacement of the S atom in OCS by a more electronegative O atom. In the most simplistic picture, this replacement would increase the partial positive charge on the carbon atom of CO<sub>2</sub> and hence enhance the electrostatic interaction between it and the ether oxygen atom.

The present paper describes a determination of the structure of the DME–CO<sub>2</sub> complex from the ground-state moments of inertia and an estimation of the binding energy of DME–CO<sub>2</sub> in the gas-phase calculated from the rotational spectroscopic parameters. In addition, we present our own ab initio results on the DME–CO<sub>2</sub> complex and comparisons with DME–OCS and complexes containing C–H hydrogen bonding interactions will be made.

## Experimental Section

The rotational spectra of the normal and four isotopically substituted forms of the DME–CO<sub>2</sub> dimer were measured in the frequency range 6–15 GHz on a Balle–Flygare type<sup>12</sup> Fourier transform microwave spectrometer. The  $J = 2 \leftarrow 1$ ,  $K_a = 0$  and  $K_a = 1$   $a$ -type transitions were readily observed during the search for the DME–OCS complex (at a signal-to-noise ratio of 20–30 in 100 gas pulses), presumably due to a CO<sub>2</sub> impurity in the OCS. Upon re-searching the 6–8 GHz region with a sample consisting only of DME and CO<sub>2</sub>, these transitions increased in intensity by about a factor of 10, giving a signal-to-noise measurement in excess of 100 for the  $2_{02} \leftarrow 1_{01}$  transition. Stark effect experiments were carried out by the

\* Corresponding author. Phone: (217) 581-2679. Fax: (217) 581-6613. E-mail: sapeebles@eiu.edu.

application of voltages of up to  $\pm 5$  kV to a pair of steel mesh plates, separated by about 30 cm and located within the Fabry–Pérot cavity of the spectrometer and easily confirmed the assignment of the most intense  $J = 2 \leftarrow 1$  transitions. Electric field calibration was performed by the measurement of the  $J = 1 \leftarrow 0$ ,  $M = 0$  transition for the OCS molecule and assuming a dipole moment of 0.71521 D.<sup>13</sup>

Samples were prepared by condensing approximately 1.5% DME (99%, Sigma-Aldrich) and 1.5% CO<sub>2</sub> (99.8%, Sigma-Aldrich) into a 2 L glass sample bulb and mixing with “first run” He/Ne (17.5% He, 82.5% Ne, BOC Gases) to give a total pressure of 1.5–2 bar. This gas mixture was expanded through a General Valve series 9 solenoid valve (with a 0.8 mm orifice) into the evacuated spectrometer chamber at a repetition frequency of 10 Hz. The frequencies of the observed rotational transitions were reproducible to better than 4 kHz. The rotational spectra of all isotopically substituted species [(<sup>13</sup>CH<sub>3</sub>)(<sup>12</sup>CH<sub>3</sub>)O–CO<sub>2</sub>, (CH<sub>3</sub>)<sub>2</sub>O–<sup>13</sup>CO<sub>2</sub>, (CH<sub>3</sub>)<sub>2</sub>O–C<sup>18</sup>O<sup>16</sup>O, (CH<sub>3</sub>)<sub>2</sub><sup>18</sup>O–C<sup>16</sup>O<sub>2</sub>] were measured in natural abundance, although the existence of the C<sub>2</sub> axis effectively doubled the abundance of the <sup>13</sup>C substitution on the DME and the <sup>18</sup>O substitution on the CO<sub>2</sub>. Since the isotopic species transitions were considerably less intense than those of the normal species, they required averaging for several thousand gas pulses to obtain good signal-to-noise; we therefore assign a higher uncertainty of 8 kHz to these transitions due to the significantly poorer quality lines. The least intense isotopic transitions (for the (CH<sub>3</sub>)<sub>2</sub><sup>18</sup>O–CO<sub>2</sub> species, which has approximately 0.20% natural abundance) were comparable in signal power to background noise levels and required averaging for up to 20 000 gas pulses for reliable frequency measurements.

## Results and Discussion

**I. Spectra.** The rotational spectrum of the normal isotopomer of the DME–CO<sub>2</sub> complex consisted of *a*-type transitions only, as would be expected for this C<sub>2v</sub> symmetry species. Although single isotopic substitution of a carbon atom in DME or of an oxygen atom in CO<sub>2</sub> results in a slight tilt of the principal inertial axes, it was not possible to observe any *b*-type transitions in these isotopomers given the very small expected  $\mu_b$  component of the dipole moment (predicted to be 0.02–0.03 D) and the already low intensity of the isotopic transitions. The short microwave pulse duration ( $\sim 0.3$   $\mu$ s) that was required for optimum signal intensity indicates a relatively large *a*-dipole moment component. The full-width at half-maximum height of the transitions was typically  $\sim 30$  kHz, although the transitions measured at higher frequencies (above about 12 GHz) were somewhat wider (up to  $\sim 50$  kHz). The transitions seemed to be a little broader than is typically seen on our instrument, and it is possible that some unresolved splittings were present, perhaps due to internal rotation of the methyl groups of DME. Attempts to analyze these transitions at higher resolution using the axial nozzle arrangement on our spectrometer still did not yield any resolvable internal rotation splittings. In any case, the increased Doppler broadening at higher frequencies was readily apparent.

Rotational transitions for the isotopic species were located within 1 MHz of the predicted frequencies by utilizing calculated isotopic rotational constant shifts obtained from an MP2/6-311++G(2d,2p) optimized structure of DME–CO<sub>2</sub> (to be discussed in Section IV). Rotational transition frequencies were fitted to a Watson *A*-reduced Hamiltonian in the *I'* representation<sup>14</sup> using the SPFIT program of Herb Pickett;<sup>15</sup> a list of the observed frequencies and the residuals from the last cycle of

**TABLE 1: Transition Frequencies for the Normal Isotopic Species of the DME–CO<sub>2</sub> Dimer**

$J'_{K_a K_c}$	$J''_{K_a K_c}$	$\nu_{\text{obs}}/\text{MHz}$	$\Delta\nu/\text{MHz}^a$
2 <sub>12</sub>	1 <sub>11</sub>	6491.2421	–0.0013
2 <sub>02</sub>	1 <sub>01</sub>	6953.8127	–0.0010
2 <sub>11</sub>	1 <sub>10</sub>	7525.9576	–0.0002
3 <sub>13</sub>	2 <sub>12</sub>	9704.1515	0.0002
3 <sub>03</sub>	2 <sub>02</sub>	10297.5499	0.0019
3 <sub>22</sub>	2 <sub>21</sub>	10512.6910	0.0018
3 <sub>21</sub>	2 <sub>20</sub>	10727.9033	–0.0007
3 <sub>12</sub>	2 <sub>11</sub>	11252.4895	–0.0002
4 <sub>14</sub>	3 <sub>13</sub>	12882.6774	0.0006
4 <sub>04</sub>	3 <sub>03</sub>	13502.2363	–0.0010
4 <sub>23</sub>	3 <sub>22</sub>	13973.9198	–0.0009
4 <sub>22</sub>	3 <sub>21</sub>	14488.2072	0.0002
4 <sub>13</sub>	3 <sub>12</sub>	14930.1041	0.0003

<sup>a</sup>  $\Delta\nu$  is given by  $\nu_{\text{obs}} - \nu_{\text{calc}}$  where  $\nu_{\text{calc}}$  is calculated from the spectroscopic parameters in Table 2.

the least-squares fit for the normal isotopomer are given in Table 1, and the resulting spectroscopic parameters are listed in Table 2. Tables of isotopic transition frequencies are given in the Supporting Information. The *A* rotational constant is not as well determined as the other rotational constants due to the lack of observed *b*- and *c*-type transitions. For the transitions belonging to the four isotopically labeled species it was necessary to fix some of the centrifugal distortion constants at the values obtained from the least-squares fitting of the normal isotope spectrum. Note that the *A* rotational constants for the <sup>13</sup>CO<sub>2</sub> and <sup>18</sup>O–DME species are very close to the *A* rotational constant for the parent isotopomer due to the location of the substituted atoms on the complex *a*-axis.

**II. Structure and Binding.** The heavy atom plane of symmetry is confirmed by an inspection of the second moments of the various isotopomers of the DME–CO<sub>2</sub> complex. Table 2 shows an invariance in the  $P_{cc}$  second moment ( $P_{cc} = \sum_i m_i c_i^2 = 0.5(I_a + I_b - I_c)$ ). The  $P_{cc}$  values for all five isotopic species are effectively constant at  $3.25 \pm 0.01$  u  $\text{\AA}^2$ , suggesting that all isotopic substitutions occur in the *ab* plane. The similarity of  $P_{cc}$  for the dimer to the literature value of  $P_{cc}$  for the DME monomer ( $= 3.2073$  u  $\text{\AA}^2$ )<sup>16</sup> confirms the location of the CO<sub>2</sub> in the DME heavy atom plane. The small difference between monomer and dimer values can be attributed to large amplitude motions within this floppy complex. The existence of the C<sub>2</sub> axis is confirmed by examination of the  $P_{bb}$  moments for the complex. A C<sub>2v</sub> structure should have  $P_{bb}(\text{complex}) \approx P_{aa}(\text{DME}) + P_{aa}(\text{CO}_2)$ ; using literature values of the rotational constants and structures for DME<sup>16</sup> and CO<sub>2</sub>,<sup>17</sup> gives  $P_{bb}(\text{complex}) = 90.241$  u  $\text{\AA}^2$  (close to the value of 90.316 u  $\text{\AA}^2$  obtained for the normal species (Table 2)). An absence of observable *b*- and *c*-type transitions further supports the C<sub>2v</sub> structure. It should be noted that exchange of the two equivalent oxygen atoms in CO<sub>2</sub> and two equivalent carbon atoms in DME as well as three pairs of hydrogen atoms should lead to an intensity variation due to nuclear spin statistics. The odd *K* lines are expected to be weighted 28 and the even *K* lines are expected to be weighted 36, to give an overall 7:9 intensity ratio for odd:even *K* transitions.<sup>18</sup> Since intensities are difficult to measure precisely on an FT-microwave spectrometer, and the nuclear spin weights for the even and odd *K* lines are so similar, no attempts were made to confirm the C<sub>2</sub> axis via intensity measurements.

Determination of the vibrationally averaged ( $r_0$ ) structure was carried out by least-squares fitting the structural parameters to the measured moments of inertia using the STRFITQ program of Schwendeman.<sup>19</sup> Since the complex possesses a C<sub>2</sub> axis and

**TABLE 2: Fitted Spectroscopic Parameters for the Five Isotopomers of the DME–CO<sub>2</sub> Dimer<sup>a</sup>**

parameter	normal	<sup>13</sup> C <sub>1</sub>	<sup>13</sup> C <sub>5</sub>	<sup>18</sup> O <sub>2</sub>	<sup>18</sup> O <sub>4</sub>
<i>A</i> /MHz	5401.240(107)	5401.475(36)	5325.538(34)	5258.154(52)	5400.997(44)
<i>B</i> /MHz	2010.8637(17)	1989.5619(8)	1984.4834(8)	1967.9844(9)	1993.6242(8)
<i>C</i> /MHz	1493.4844(15)	1481.7055(8)	1473.1278(8)	1458.8604(11)	1484.0309(6)
$\Delta_J$ /kHz	2.61(4)	2.612(22)	2.577(22)	2.646(36)	[2.61]
$\Delta_{JK}$ /kHz	3.07(18)	2.77(17)	2.66(17)	2.30(25)	[3.07]
$\Delta_K$ /kHz	−149(30)	[−149] <sup>b</sup>	[−149]	[−149]	[−149]
$\delta_J$ /kHz	0.691(29)	[0.691]	[0.691]	[0.691]	[0.691]
<i>N</i> <sup>c</sup>	13	13	13	10	8
$\Delta\nu_{\text{rms}}$ /kHz <sup>d</sup>	0.97	3.48	2.96	3.56	2.00
<i>P</i> <sub>aa</sub> /amu Å <sup>2</sup> <sup>e</sup>	248.0732(7)	250.7657(2)	251.4167(2)	253.5537(3)	250.2355(3)
<i>P</i> <sub>bb</sub> /amu Å <sup>2</sup>	90.3160(10)	90.3136(4)	91.6486(3)	92.8667(5)	90.3093(4)
<i>P</i> <sub>cc</sub> /amu Å <sup>2</sup>	3.2512(9)	3.2496(3)	3.2486(3)	3.2466(4)	3.2621(4)

<sup>a</sup> Atom numbering is given in Figure 1. Uncertainties in parentheses are a priori errors as reported from the SPFIT program. Absolute errors may be obtained by multiplication of these errors by a factor ( $\Delta\nu_{\text{rms}}/4$  kHz) where 4 kHz is the assumed error in frequency measurement used in the fitting program. <sup>b</sup> Distortion constants in square brackets were fixed at the values for the normal isotopomer. <sup>c</sup> *N* is the number of fitted transitions. <sup>d</sup>  $\Delta\nu_{\text{rms}}$  is the root-mean-square deviation of the fit,  $\Delta\nu_{\text{rms}} = (\sum (\nu_{\text{obs}} - \nu_{\text{calc}})^2/N)^{1/2}$ . <sup>e</sup> *P*<sub>aa</sub>, *P*<sub>bb</sub>, and *P*<sub>cc</sub> are the second moments as defined in the text.

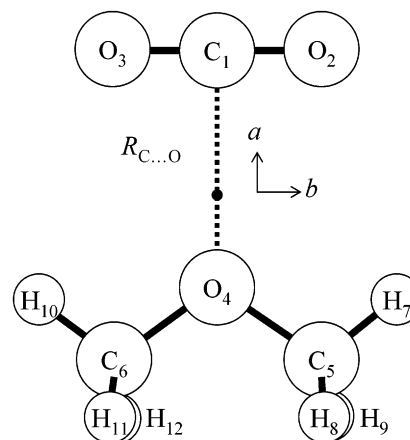
**TABLE 3: Structural Parameters for the DME–CO<sub>2</sub> Complex Obtained from the Least-Squares Fitting of the Moment of Inertia Data and from the ab Initio Calculations**

	<i>R</i> <sub>C...O</sub> /Å	<i>R</i> <sub>cm</sub> <sup>b</sup> /u Å <sup>2</sup>	$\Delta I_{\text{rms}}$ <sup>c</sup> /u Å <sup>2</sup>
Fits of Single Isotopomer Data <sup>a</sup>			
normal	2.7114(13)	3.2562(13)	0.2619
<sup>13</sup> C <sub>5</sub> or <sup>13</sup> C <sub>6</sub>	2.7111(13)	3.2559(13)	0.2720
<sup>13</sup> C <sub>1</sub>	2.7110(12)	3.2558(12)	0.2613
<sup>18</sup> O <sub>2</sub> or <sup>18</sup> O <sub>3</sub>	2.7111(12)	3.2559(12)	0.2601
<sup>18</sup> O <sub>4</sub>	2.7115(12)	3.2563(12)	0.2494
Fits of All Isotopic Data <sup>d</sup>			
fit <i>I</i> <sub>a</sub> , <i>I</i> <sub>b</sub>	2.7100(11)	3.2548(11)	0.3511
fit <i>I</i> <sub>a</sub> , <i>I</i> <sub>c</sub>	2.7125(11)	3.2573(11)	0.3509
fit <i>I</i> <sub>b</sub> , <i>I</i> <sub>c</sub>	2.7112(4)	3.2560(4)	0.1972
fit <i>I</i> <sub>a</sub> , <i>I</i> <sub>b</sub> , <i>I</i> <sub>c</sub>	2.7112(7)	3.2560(7)	0.3223
best <sup>e</sup>	2.711(1)	3.256(1)	—
ab initio <sup>f</sup>	2.685	3.221	—

<sup>a</sup> Since only a single structural parameter is fit it is possible to obtain a value of the *R*<sub>C...O</sub> distance for each isotopic species. Results of fitting *I*<sub>b</sub> and *I*<sub>c</sub> for the single isotopic species are shown. Substituted atom numbers are shown in Figure 1. <sup>b</sup> *R*<sub>cm</sub> is the center of mass separation, calculated from the principal axis coordinates. <sup>c</sup>  $\Delta I_{\text{rms}}$  is the root-mean-square deviation of the least-squares fit, defined by  $\Delta I_{\text{rms}} = (\sum (I(\text{obs}) - I(\text{calc}))^2/N)^{1/2}$  where *N* is the number of moments fitted. <sup>d</sup> Fitting includes the inertial data for all isotopic species; the combination of moments included in each fit is indicated. <sup>e</sup> Estimated best values from the evaluation of all inertial fit data. <sup>f</sup> Ab initio parameters are obtained from the MP2/6-311++G(2d,2p) optimization.

a heavy atom plane of symmetry and the monomer structures are assumed to be unchanged upon complexation,<sup>16,17</sup> there remains only a single structural parameter to fit, the *R*<sub>C...O</sub> distance. It was therefore possible to obtain a value for this parameter for each of the five isotopomers. Using the *I*<sub>b</sub> and *I*<sub>c</sub> moments for each individual isotopomer, the *R*<sub>C...O</sub> distance was computed by least-squares fit. The results consistently gave a value of 2.711(1) Å (see Table 3). Fitting all 15 available moments of inertia (*I*<sub>a</sub>, *I*<sub>b</sub>, and *I*<sub>c</sub>) from the five isotopic species gave a C...O distance that agreed well with that obtained from the fits of *I*<sub>b</sub> and *I*<sub>c</sub> for each isotopomer individually and also with a fit of only *I*<sub>b</sub> and *I*<sub>c</sub> for all five isotopomers together. All derived structural parameters are given in Table 3. Fits that include *I*<sub>a</sub> give significantly higher root-mean-square deviations ( $\Delta I_{\text{rms}}$ ) due to the higher uncertainty in the *A* rotational constant and its insensitivity to *R*<sub>C...O</sub>; however, the C...O distances resulting from these fits still fall within the reported uncertainties.

The experimental intermolecular C...O distance of 2.711(1) Å is about 0.4 Å longer than the sum of the Pauling van der

**Figure 1.** The structure of the DME–CO<sub>2</sub> complex showing the atom numbering. The single adjustable parameter, *R*<sub>C...O</sub>, is indicated by the dotted line and the filled circle (●) represents the center of mass of the complex.

Waals radii<sup>20</sup> for an oxygen atom and a carbon atom (3.1 Å). This relatively short bond length seems to indicate a fairly strong binding between the DME and the CO<sub>2</sub>, this interaction presumably largely governed by electrostatic forces between the two monomers. In addition to an attractive dipole–quadrupole interaction between the DME and the CO<sub>2</sub>, the opposite signs for the *Q*<sub>aa</sub> quadrupole moments of the two monomers [*Q*<sub>aa</sub>(DME) = +2.5(4) *ea*<sub>0</sub><sup>2</sup>, *Q*<sub>aa</sub>(CO<sub>2</sub>) = −3.1(2) *ea*<sub>0</sub><sup>2</sup>]<sup>21</sup> mean that parallel alignment of the *Q*<sub>aa</sub> quadrupole moments for the two monomers is electrostatically favorable. The electric quadrupole component *Q*<sub>bb</sub> for DME (*Q*<sub>bb</sub> = −1.5(4) *ea*<sub>0</sub><sup>2</sup>),<sup>21</sup> lying parallel to the dimer *a*-axis, also interacts favorably in a T-shaped orientation with the *Q*<sub>aa</sub> moment of CO<sub>2</sub>.

It is informative to compare some intermolecular distances involving the methyl hydrogen atoms (see Figure 1 for the assumed methyl group orientation). The distance from the oxygen atoms of CO<sub>2</sub> to the nearest H of DME will be primarily governed by the intermolecular C...O interaction which is already considerably shorter (2.711(1) Å) than the sum of van der Waals radii (3.1 Å<sup>20</sup>); however, any secondary attractive C–H...O hydrogen bonding interactions would serve to pull the monomers even closer together. The H...O distance between the DME and the CO<sub>2</sub> derived from the inertial fit is 2.964(2) Å, certainly longer than the sum of the van der Waals radii of oxygen and hydrogen (2.6 Å), but within the wide range of distances seen for a C–H...O interaction.<sup>22</sup> The C–H...O

**TABLE 4: Principal Axis Coordinates for DME–CO<sub>2</sub> (in Å) Resulting from the Inertial Fit<sup>a</sup>**

substituted atom	a	b	c
<sup>13</sup> C <sub>1</sub>	−1.6651 [1.6473]	0.0000 [0.0000]	0.0000 [0.0000]
<sup>13</sup> C <sub>5</sub> (or <sup>13</sup> C <sub>6</sub> )	1.8392 [1.8278]	±1.1660 [1.1711]	0.0000 [0.0000]
<sup>18</sup> O <sub>2</sub> (or <sup>18</sup> O <sub>3</sub> )	−1.6651 [1.6584]	±1.1620 [1.1603]	0.0000 [0.0000]
<sup>18</sup> O <sub>4</sub>	1.0461 [1.0502]	0.0000 [0.0000]	0.0000 [0.0751] <sup>b</sup>

<sup>a</sup> The values in brackets are the coordinates derived from the Kraitchman single isotopic substitution data. See Figure 1 for atom numbering. Propagated uncertainties in the Kraitchman coordinates are calculated to be ±0.0001 Å or less. <sup>b</sup> The relatively poor agreement of the Kraitchman coordinate with the inertial fit coordinate for this atom may be attributed to the increased uncertainty in determining substitution coordinates that have near-zero values (since Kraitchman's equations actually fit the square of the coordinate). In addition, the data set for the <sup>18</sup>O<sub>4</sub> species is the smallest of those measured, leading to the least well-determined rotational constants.

interaction in DME–CO<sub>2</sub> is also highly nonlinear ( $\alpha(\text{C–H}\cdots\text{O}) = 111.3^\circ$ ), making this interaction quite different from conventional, nearly linear, hydrogen bonds, but it still falls within the upper bounds of C–H hydrogen bonding interactions.<sup>22</sup>

Single isotopic substitution of all heavy atoms in this complex also allowed a calculation of the O $\cdots$ C distance by using Kraitchman's equations<sup>23</sup> to determine the principal axis coordinates of the substituted atoms. This served as a confirmation of the consistency of the inertial fit structure. The principal axis coordinates resulting from the least-squares inertial fit are given in Table 4 along with the coordinates obtained from the Kraitchman single substitution calculations.  $R_{\text{C}\cdots\text{O}}$  is calculated to be 2.6975(2) Å from the O and C Kraitchman coordinates of the DME and CO<sub>2</sub>, in reasonable agreement with the inertial fit value of 2.711(1) Å. Note that the C=O bond length calculated from the Kraitchman coordinates is 1.1604(2) Å, in excellent agreement with the literature value of the monomer (1.162 Å<sup>17</sup>); this distance was held fixed at the literature value during the inertial fit. Likewise, the C–O distance of DME in the dimer (computed from the Kraitchman coordinates) is 1.4058(3) Å, within 0.005 Å of the literature value of 1.410 Å.<sup>16</sup> The agreement between these parameters and the literature values supports the assumption that the monomer geometries are effectively unchanged upon complexation. It is also possible to use the substitution coordinates to calculate an O=C=O angle of CO<sub>2</sub> of 178.9(5)°, with the oxygen atoms bent away from the DME molecule. This is in qualitative agreement with the distortion of the CO<sub>2</sub> monomer predicted by the ab initio calculations (see Section IV).

In light of the recent characterization of the structurally similar DME–OCS complex, numerous comparisons between these two species are possible. The experimental  $R_{\text{C}\cdots\text{O}}$  distance of 2.711(1) Å in the DME–CO<sub>2</sub> complex is almost exactly 0.2 Å shorter than the value of 2.916(3) Å seen in the DME–OCS complex, presumably since the CO<sub>2</sub> molecule can approach slightly closer to the DME than can the OCS with the bulkier S atom. An inspection of the intermolecular distances in the  $r_0$  structure of DME–OCS reveals that the O $\cdots$ O and O $\cdots$ S distances (from the ether oxygen atom to the oxygen and sulfur atoms of the OCS) are 3.014(8) Å and 3.463(3) Å, respectively. These values are 0.214 Å and 0.213 Å more than the sum of the O $\cdots$ O and O $\cdots$ S van der Waals radii, respectively, and interestingly they differ by the same amount as the difference in the sums of the van der Waals radii<sup>20</sup> for the O and S atoms (~0.45 Å),

indicating the tilt of the OCS is explainable by steric factors. For DME–CO<sub>2</sub> the O $\cdots$ O distances (between the oxygen atoms of CO<sub>2</sub> and the ether oxygen atom) are both 2.950(2) Å, about 0.15 Å greater than the sum of the van der Waals radii.

In complexes in which the van der Waals bond lies approximately along the *a*-axis it is possible to obtain an estimate of the stretching force constant for the weak bond ( $k_s$ ) and the binding energy ( $E_B$ ) of the complex in the pseudodiatomic approximation using the expressions<sup>24,25</sup>

$$k_s = \frac{16\pi^4(\mu R_{\text{cm}})^2[4B^4 + 4C^4 - (B - C)^2(B + C)^2]}{hD_J} \quad (1)$$

and

$$E_B = \left(\frac{1}{72}\right)k_s R_{\text{cm}}^2 \quad (2)$$

where  $\mu$  is the reduced mass of the complex,  $R_{\text{cm}}$  is the center of mass separation,  $B$  and  $C$  are the rotational constants of the complex, and  $D_J$  is the quartic distortion constant in Watson's *S*-reduction Hamiltonian<sup>14</sup> (which in the present case is numerically equal to the  $\Delta_J$  distortion constant); all of the parameters in eqs 1 and 2 must be in SI units. Equation 2 is derived by assuming a Lennard–Jones-type potential function and although only a crude approximation to the true intermolecular interaction potential it does allow comparisons of binding energies to be made between similar complexes. Our experimental results give a value of  $E_B$  of 9.7(2) kJ mol<sup>−1</sup> for the DME–CO<sub>2</sub> complex and 7.1(2) kJ mol<sup>−1</sup> for the DME–OCS complex,<sup>9</sup> with force constants of 10.9(2) N m<sup>−1</sup> and 6.7(2) N m<sup>−1</sup>, respectively (see Table 5). This confirms that the DME–CO<sub>2</sub> complex is slightly more strongly bound than DME–OCS, as might be expected from purely electrostatic arguments when the sulfur atom of OCS is replaced with a more electronegative oxygen atom. Also, the quadrupole moment of OCS is −0.65(11)  $ea_0^2$ , about one-quarter as large as the quadrupole moment of CO<sub>2</sub>,<sup>21</sup> and implying weaker quadrupole–quadrupole interactions than are present in the DME–CO<sub>2</sub> complex. Comparison with the DME dimer,<sup>1</sup> DME–1,1-difluoroethylene<sup>2</sup> and DME–trifluoroethylene<sup>2</sup> complexes (Table 6) shows that  $E_B$  for DME–CO<sub>2</sub> is between 1.5 and 2 times as large as that for the DME complexes that contain only C–H hydrogen bonding interactions. The only binding energy in Table 6 that is comparable in magnitude to that observed for DME–CO<sub>2</sub> is the value for DME–HF, a “true” hydrogen bonded complex (possessing an O $\cdots$ H–F interaction) which has an estimated binding energy of about 9(2) kJ/mol. It should be noted that this  $E_B$  value has been computed based on the  $R_{\text{cm}}$  separation obtained from the ab initio structure for DME–HF reported in ref 4 and hence is subject to rather larger uncertainties than for the other species listed in Table 6.

**III. Dipole Moment.** Stark effect measurements for the DME–CO<sub>2</sub> complex typically showed very fast shifts since the single dipole component is oriented along the *a*-axis and is expected to be fairly sizable (based on the DME monomer moment of 1.31 D<sup>26</sup>). Table 7 lists the observed and calculated Stark coefficients along with the fitted value of the  $\mu_a$  dipole component. Calculated Stark coefficients were computed by second order perturbation theory using the rotational constants for the normal isotopomer that are listed in Table 2. As a result of the large Stark coefficients, the electric field calibration was somewhat troublesome since OCS, which was used for the calibration, has relatively small shifts at voltages of less than about 1000 V; therefore, the transitions that were chosen for

**TABLE 5: Comparison of Experimental and ab Initio Binding Energies and Rotational Constants for DME–OCS and DME–CO<sub>2</sub>**

	DME–OCS		DME–CO <sub>2</sub>	
	experiment	ab initio <sup>c</sup>	experiment	ab initio <sup>c</sup>
$k_s/\text{N m}^{-1}$ <sup>a</sup>	6.7(2)	–	10.9(2)	–
$E_B/\text{kJ mol}^{-1}$ <sup>b</sup>	7.1(2)	7.3	9.7(2)	10.8
MP2 energy/ $E_h$ <sup>d</sup>	–	–665.482055	–	–342.917149
$A/\text{MHz}$	4069.4106(23)	4065	5401.240(107)	5379
$B/\text{MHz}$	1431.7413(7)	1450	2010.8637(17)	2018
$C/\text{MHz}$	1074.2925(5)	1083	1493.4844(15)	1495

<sup>a</sup>  $k_s$  is the weak bond stretching force constant (calculated as described in the text using the pseudodiatomic approximation). <sup>b</sup> Binding energy of the complex calculated using eq 2. The ab initio binding energy includes corrections for BSSE and for ZPE, as described in the text. <sup>c</sup> Optimized at the MP2/6-311++G(2d,2p) level using Gaussian 98. <sup>d</sup> Total electronic energy (not BSSE corrected) at the MP2/6-311++G(2d,2p) level.

**TABLE 6: Comparison of Force Constants and Binding Energies (calculated from the spectroscopic parameters) for Several DME Complexes**

complex	$k_s/\text{N m}^{-1}$	$E_B/\text{kJ mol}^{-1}$	ref
DME–Ne	1.0	1.0	5
DME–Ar	2.3	2.5	6
DME–Kr	2.6	2.9	7
DME–Xe	3.0	3.7	8
DME–DFE <sup>a</sup>	3.55	4.76	2
DME–TFE <sup>a</sup>	4.45	5.98	2
DME–DME	4.7	5.7	1
DME–OCS	6.7(2)	7.1(2)	9
DME–CO <sub>2</sub>	10.9(2)	9.7(2)	this work <sup>c</sup>
DME–HF	12(2) <sup>b</sup>	9(2) <sup>b</sup>	4

<sup>a</sup> DFE = 1,1-difluoroethylene, TFE = 1,1,2-trifluoroethylene. <sup>b</sup> Estimated from the structure given in Table 5 of ref 4 ( $R_{\text{O}\cdots\text{H}} = 1.64$  Å,  $\tau = 40^\circ$ ,  $\alpha = 178.5^\circ$ ). If  $R_{\text{O}\cdots\text{H}} = 1.68$  Å (which provides better agreement with measured rotational constants), then  $k_s = 12.7$  N m<sup>−1</sup> and  $E_B = 9.4$  kJ mol<sup>−1</sup>. See the text for further details. <sup>c</sup> Reference 10 reports a value of  $-16.5(5)$  kJ mol<sup>−1</sup> for the gas-phase complexation energy for DME–CO<sub>2</sub> (converted from the standard enthalpy of complexation in liquid Ar).

**TABLE 7: Experimental and Calculated Stark Coefficients and Dipole Moment for the DME–CO<sub>2</sub> Complex**

transition <sup>a</sup>	$ M $	$\Delta\nu/E^2$ (obs) <sup>b</sup>	$\Delta\nu/E^2$ (calc) <sup>b</sup>	% difference <sup>c</sup>
$2_{02} \leftarrow 1_{01}$	1	2.4875	2.4644	0.94
$2_{12} \leftarrow 1_{11}$	0	2.6126	2.6620	−1.9
$2_{11} \leftarrow 1_{10}$	0	2.3069	2.2964	0.46
$3_{03} \leftarrow 2_{02}$	0	−0.5400	−0.5140	5.1
$3_{03} \leftarrow 2_{02}$	1	−0.1610	−0.1496	7.6
$3_{03} \leftarrow 2_{02}$	2	0.9813	0.9436	4.0

$\mu_a = \mu_{\text{total}} = 1.661(6)$  D

<sup>a</sup> The  $M = 0$  component for the  $2_{02} \leftarrow 1_{01}$  transition showed some curvature in the plot while the  $M = 1$  lobes for the  $2_{12} \leftarrow 1_{11}$  and  $2_{11} \leftarrow 1_{10}$  transitions had particularly fast Stark shifts; hence these components are excluded from the fit. <sup>b</sup> Observed and calculated Stark coefficients are in units of  $10^{-5}$  MHz/(V<sup>2</sup> cm<sup>−2</sup>). <sup>c</sup> % difference is given by  $\{[\Delta\nu/E^2(\text{obs}) - \Delta\nu/E^2(\text{calc})]/[\Delta\nu/E^2(\text{calc})]\} \times 100$ .

study were among the slowest moving to ensure reasonable frequency shifts in the region where the electric field calibration is most reliable. Attempts to include the  $\mu_b$ - and  $\mu_c$ -dipole moment components in the least-squares fit, either alone or in various combinations with the  $\mu_a$ -dipole component, resulted in significantly poorer quality fits, but changes in the value of  $\mu_a$  were insignificant compared to the reported uncertainties. Measured Stark shifts were all less than 1 MHz and no deviation from linearity in the  $\Delta\nu$  vs  $E^2$  plots was observed for any of the transitions listed in Table 7.

It is interesting to compare the dipole moment in this complex with that of the DME monomer (1.31 D).<sup>26</sup> The dipole moment of the dimer shows an increase of around 0.35 D upon complexation with CO<sub>2</sub>. This could arise from a distortion of CO<sub>2</sub> and/or a shift of electron density into the intermolecular

region upon complex formation. The first possibility can be explored using the results from the MP2 ab initio optimization which shows that the oxygen atoms of the CO<sub>2</sub> are distorted slightly away from the DME, although the deviation from linearity is small (O=C=O angle 177.6°). This only amounts to a calculated 0.05 D enhancement of the dipole moment; therefore, the majority of the dipole moment enhancement must be attributable to a charge redistribution. A detailed investigation of this possibility by ab initio techniques is beyond the scope of this study. The ab initio values can be used to predict the dipole moment change upon complexation. The optimized DME–CO<sub>2</sub> complex is calculated to have a dipole of 1.83 D while the isolated optimized DME monomer has a predicted dipole of 1.43 D, giving an enhancement of 0.40 D upon formation of the DME–CO<sub>2</sub> dimer. Although the individual dipole moments are overestimated by about 10%, the magnitude and direction of the predicted dipole moment increase upon complexation are in reasonable agreement with the measured enhancement of 0.35 D.

**IV. Ab Initio Calculations.** Theoretical calculations were carried out on the DME–CO<sub>2</sub> complex using the Gaussian 98 suite of programs. G98W<sup>27</sup> was used on a 2.8 GHz Gateway E6000 Series PC to optimize the geometry of the  $C_{2v}$  structure at levels up to second-order Møller–Plesset perturbation theory, MP2 (frozen core). Vibrational frequency calculations, carried out on a 500 MHz Alpha PC 264DP workstation running Tru64 Unix and Gaussian 98,<sup>28</sup> were used to confirm the nature of the minimum on the potential energy surface. Basis set superposition error (BSSE) corrections to the interaction energy were carried out using the method described by Xantheas, which includes fragment relaxation energy terms.<sup>29</sup> This method of correcting for BSSE includes the relatively small energy terms which arise from distorting the monomers from their isolated geometries to the geometries observed in the dimer. Zero point energy (ZPE) corrections were also included in the calculations of the interaction energy. No attempts to correct the potential energy surface for BSSE during geometry optimization were made in the present work, although previous studies on hydrogen bonded systems have shown that this type of correction can be expected to increase the predicted intermolecular bond length somewhat.<sup>11</sup>

Location of the rotational spectra of the isotopic species was simplified by calculating isotopic shifts using a model derived from an ab initio MP2/6-311++G(2d,2p) optimization of the DME–CO<sub>2</sub> complex. Previous ab initio calculations on this complex<sup>10</sup> indicated that numerous different starting orientations of the two monomers consistently converged to the same  $C_{2v}$  structure. Hence, our initial structure was based on a  $C_{2v}$  form of the dimer and a detailed investigation of the PES to identify other higher energy geometries was not repeated in the current work.

The predicted  $C_{2v}$  structure for this dimer gave very good agreement with the experimental structural parameters; both theoretical and experimental parameters are listed in Table 3. Table 3 shows that the MP2 calculation predicts a C···O intermolecular bond distance of 2.685 Å, underestimating the experimental distance of 2.711(1) Å by less than 0.03 Å. This underestimate is similar to the value of approximately 0.05 Å obtained from the ab initio prediction of the C···O distance for the DME–OCS complex.<sup>9</sup> It should be pointed out that the ab initio optimized structure provides an equilibrium value of the bond length ( $r_e$ ), while the experimentally determined value is a ground-state averaged value ( $r_0$ ) and these quantities could be expected to differ by a few hundredths of an angstrom due to the different natures of the parameters being determined. The CO<sub>2</sub> monomer is predicted to be slightly nonlinear with a bend of the oxygen atoms of about 2.4° away from the DME. The direction of this distortion is consistent with that obtained from the Kraitchman coordinates although the value is larger than the 1.1° derived from the principal axis coordinates. A comparison of the experimental and theoretical rotational constants is given in Table 5 which also lists the interaction energy, determined both from the spectroscopic parameters (see Section II) and from the ab initio calculations. Tables 5 and 6 show that the ab initio binding energy for DME–CO<sub>2</sub> (10.8 kJ mol<sup>-1</sup>) is in reasonable agreement with the value obtained from the pseudodiatomic model (9.7(2) kJ mol<sup>-1</sup>), although both our experimental and theoretical values are significantly smaller than the value of 16.5(5) kJ mol<sup>-1</sup> obtained from an extrapolation of the  $\Delta_{\text{complex}}H^\circ$  value from the IR study to a gas-phase complexation energy.<sup>10</sup>

The shorter predicted bond length in the DME–CO<sub>2</sub> calculations (compared to the DME–OCS complex) can be at least partially explained by an inspection of the Mulliken atomic charges on the carbon atoms of the OCS or CO<sub>2</sub>. At this level of theory for the CO<sub>2</sub> monomer the Mulliken atomic charge on carbon is calculated to be +0.41 while for OCS it is +0.20. This is consistent with the intuitive reasoning that replacement of the S atom in OCS by the more electronegative oxygen in CO<sub>2</sub> increases the electrophilic character of the carbon atom and hence increases the strength of binding between the DME and the CO<sub>2</sub>, giving a higher binding energy and shorter bond length.

As already mentioned, in contrast to the previous ab initio study,<sup>10</sup> our ab initio calculations did not explicitly include BSSE corrections to the potential energy surface during the optimizations. For a comparison with the BSSE corrected results of van Ginderen, et al.<sup>10</sup> we also carried out an optimization at their MP2/6-311++G(d,p) level but without including the BSSE corrections. This calculation gave almost the same distance as we obtained with the slightly larger basis set ( $R_{\text{C}\cdots\text{O}}$  distance of 2.687 Å vs 2.685 Å with the larger basis) and vibrational frequencies that differed by a few tenths of wavenumbers when compared to the previous ab initio results.<sup>10</sup> This illustrates the sensitivity of the vibrational frequencies to the level of calculation and to the “tightness” of the optimization procedure as well as to the inclusion of BSSE effects on the potential energy surface. Obviously neglect of BSSE tends to give slightly shorter bond lengths and in the case of DME–CO<sub>2</sub> the treatment of BSSE slightly overestimates the C···O distance.<sup>10</sup>

## Conclusions

The rotational spectra of five isotopomers of the weakly bound complex DME–CO<sub>2</sub> have been assigned and have allowed the determination of a heavy-atom planar  $C_{2v}$  structure,

in which the CO<sub>2</sub> lies perpendicular to the  $C_2$  axis of DME. Since the complex possesses  $C_{2v}$  symmetry, only a single structural parameter (the C···O distance) needs to be determined. The value obtained for this distance is 2.711(1) Å, about 0.2 Å shorter than the C···O distance observed in the closely related DME–OCS complex.<sup>9</sup> The O···C distance may be compared to the value obtained from ab initio calculations by van Ginderen, et al. of 2.812 Å,<sup>10</sup> where the BSSE corrected value is found to be too long by 0.1 Å, suggesting a slight overcorrection of the bond length from BSSE effects. The ab initio calculations carried out in the present work at the MP2/6-311++G(2d,2p) level (not including BSSE corrections to the potential energy surface) give a much closer value of 2.685 Å, although this agreement is clearly somewhat fortuitous. Similarly good quality agreement was seen in the DME–OCS complex, where the predicted C···O distance of 2.864 Å was within 0.05 Å of the experimental determination of 2.916(3) Å. The C···O distances for the two complexes were underestimated by about the same extent at this level of calculation, and this provides a useful correction for application to similar systems optimized at the same level and basis.

Inspection of the binding energies highlights that the bonding in DME–CO<sub>2</sub> is stronger than in many complexes of DME. This fact, taken along with the observed blue shifts in the C–H stretching modes in the IR work,<sup>10</sup> might be taken as evidence, but not conclusive proof, of some C–H···O interaction taking place. High level ab initio electron density maps would presumably help to further elucidate the nature of the bonding in DME–CO<sub>2</sub> and related complexes, as well as give information on the charge redistribution that accompanies the increase in dipole moment on complex formation.

**Acknowledgment.** Acknowledgment is made to the donors of the American Chemical Society Petroleum Research Fund for support of this research (PRF grant #39752-GB6). The authors also thank Jim Wentz of the University of Illinois Urbana-Champaign for modification and installation of the high voltage connectors and Roy Wentz of the Glassblowing Shop in the Department of Chemistry at the University of Michigan for constructing the high vacuum line used for sample preparation.

**Supporting Information Available:** Tables of measured transition frequencies for the four isotopic species. This material is available free of charge via the Internet at <http://pubs.acs.org>

## References and Notes

- (1) Tatamitani, Y.; Liu, B.; Shimada, J.; Ogata, T.; Ottaviani, P.; Maris, A.; Caminati, W.; Alonso, J. *J. Am. Chem. Soc.* **2002**, *124*, 2739.
- (2) Tatamitani, Y.; Ogata, T. *J. Mol. Spec.* **2003**, *222*, 102.
- (3) Caminati, W.; Melandri, S.; Moreschini, P.; Favero, P. *G. Angew. Chem., Int. Ed.* **1999**, *38*, 2924.
- (4) Ottaviani, P.; Caminati, W.; Velino, B.; Blanco, S.; Lessarri, A.; López, J.; Alonso, J. *Chem. Phys. Chem.* **2004**, *5*, 336.
- (5) Maris, A.; Caminati, W. *J. Chem. Phys.* **2003**, *118*, 1649.
- (6) Ottaviani, P.; Maris, A.; Caminati, W.; Tatamitani, Y.; Suzuki, Y.; Ogata, T.; Alonso, J. *Chem. Phys. Lett.* **2002**, *361*, 341.
- (7) Velino, B.; Melandri, S.; Caminati, W. *J. Phys. Chem. A* **2004**, *108*, 4224.
- (8) Favero, L.; Velino, B.; Millemaggi, A.; Caminati, W. *Chem. Phys. Chem.* **2003**, *4*, 881.
- (9) Newby, J. J.; Peebles, R. A.; Peebles, S. A. *J. Phys. Chem. A*, **2004**, *108*, 7372.
- (10) van Ginderen, P.; Herrebout, W. A.; van der Veken, B. J. *J. Phys. Chem. A* **2003**, *107*, 5391.
- (11) Simon, S.; Duran, M.; Dannenberg, J. J. *J. Chem. Phys.* **1996**, *105*, 11024.
- (12) Balle, T. J.; Flygare, W. H. *Rev. Sci. Instrum.* **1981**, *52*, 33.
- (13) Muentzer, J. S. *J. Chem. Phys.* **1968**, *48*, 4544.

- (14) Watson J. K. G. *J. Chem. Phys.* **1969**, *46*, 1935.
- (15) Pickett, H. M. *J. Mol. Spectrosc.* **1991**, *148*, 371.
- (16) Niide, Y.; Hayashi, M. *J. Mol. Spectrosc.* **2003**, *220*, 65.
- (17) Plyler, E. K.; Blaine, L. R.; Tidwell, E. D. *J. Res. Natl. Bur. Stand.* **1955**, *55*, 183.
- (18) Townes, C. H.; Schawlow, A. L. *Microwave Spectroscopy*; Dover Publications Inc.: New York, 1975; p 104.
- (19) Schwendeman, R. H. *Critical Evaluation of Chemical and Physical Structural Information*; Lide, D. R., Paul, M. A., Eds.; National Academy of Sciences: Washington, DC, 1974.
- (20) Pauling, L. *College Chemistry*, 3rd ed.; W. H. Freeman and Company: San Francisco, 1964; p 290.
- (21) Gray, C. G.; Gubbins, K. E. *Theory of Molecular Fluids, Vol. 1: Fundamentals*; Oxford University Press: Oxford, 1984; p 580, 592, and references therein.
- (22) See, for example, the plots of C–H···O angle against O···H distance in Steiner, T.; Saenger, W. *J. Am. Chem. Soc.* **1992**, *114*, 10146.
- (23) Kraitchman, J. *Am. J. Phys.* **1953**, *21*, 17.
- (24) Millen, D. J. *Can. J. Chem.* **1985**, *63*, 1477.
- (25) Read, W. G.; Campbell, E. J.; Henderson, G. *J. Chem. Phys.* **1983**, *78*, 3501.
- (26) Blukis, U.; Kasai, P. H.; Myers, R. J. *J. Chem. Phys.* **1963**, *38*, 2753.
- (27) Frisch, M. J.; Trucks, G. W.; Schlegel, H. B.; Scuseria, G. E.; Robb, M. A.; Cheeseman, J. R.; Zakrzewski, V. G.; Montgomery, J. A.; Stratmann, R. E.; Burant, J. C.; Dapprich, S.; Millam, J. M.; Daniels, A. D.; Kudin, K. N.; Strain, M. C.; Farkas, O.; Tomasi, J.; Barone, V.; Cossi, M.; Cammi, R.; Mennucci, B.; Pomelli, C.; Adamo, C.; Clifford, S.; Ochterski, J.; Petersson, G. A.; Ayala, P. Y.; Cui, Q.; Morokuma, K.; Malick, D. K.; Rabuck, A. D.; Raghavachari, K.; Foresman, J. B.; Cioslowski, J.; Ortiz, J. V.; Stefanov, B. B.; Liu, G.; Liashenko, A.; Piskorz, P.; Komaromi, I.; Gomperts, R.; Martin, R. L.; Fox, D. J.; Keith, T.; Al-Laham, M. A.; Peng, C. Y.; Nanayakkara, A.; Challacombe, M.; Gill, P. M. W.; Johnson, B. G.; Chen, W.; Wong, M. W.; Andres, J. L.; Head-Gordon, M.; Replogle, E. S.; Pople, J. A. *Gaussian 98W*, revision A.11); Gaussian, Inc.: Pittsburgh, PA, 1998.
- (28) Frisch, M. J.; Trucks, G. W.; Schlegel, H. B.; Scuseria, G. E.; Robb, M. A.; Cheeseman, J. R.; Zakrzewski, V. G.; Montgomery, J. A.; Stratmann, R. E.; Burant, J. C.; Dapprich, S.; Millam, J. M.; Daniels, A. D.; Kudin, K. N.; Strain, M. C.; Farkas, O.; Tomasi, J.; Barone, V.; Cossi, M.; Cammi, R.; Mennucci, B.; Pomelli, C.; Adamo, C.; Clifford, S.; Ochterski, J.; Petersson, G. A.; Ayala, P. Y.; Cui, Q.; Morokuma, K.; Malick, D. K.; Rabuck, A. D.; Raghavachari, K.; Foresman, J. B.; Cioslowski, J.; Ortiz, J. V.; Baboul, A. G.; B. B. Stefanov, B. B.; Liu, G.; Liashenko, A.; Piskorz, P.; Komaromi, I.; Gomperts, R.; Martin, R. L.; Fox, D. J.; Keith, T.; Al-Laham, M. A.; Peng, C. Y.; Nanayakkara, A.; Challacombe, M.; Gill, P. M. W.; Johnson, B. G.; Chen, W.; Wong, M. W.; Andres, J. L.; Gonzalez, C.; Head-Gordon, M.; Replogle, E. S.; Pople, J. A. *Gaussian 98*, revision A.9; Gaussian, Inc.: Pittsburgh, PA, 1998.
- (29) Xantheas, S. S. *J. Chem. Phys.* **1996**, *104*, 8821.